

Ministère de
l'Enseignement Supérieur
et de la Recherche
Scientifique
Université de Carthage
Ecole Polytechnique de
Tunisie



وزارة التعليم العالي و
البحث العلمي
جامعة قرطاج
المدرسة التونسية للتقنيات

Engineering Internship Report

Modelling of an elastomer material under a mode of deformation under uniaxial stress

3rd June - 6th September, 2024

Elaborated by :

Nour MNEJJA

Third Year Student- SYSCO

Within :



Supervised by :

Mr.Ahmed BRAHAM

Aeronautical Engineer & CAE - CAD - FEA Instructor

Academic Year

2024 - 2025

Rue Elkhawarezmi BP 743 La Marsa 2078

Tel: 71 774 611 – 71 774 699 Fax: 71 748 843

Site Web: www.ept.tn

نهج الخوارزمي صب 743 المرسى 2078

الهاتف: 71 774 611 - 71 774 699 الفاكس: 71 748 843

موقع الويب: www.ept.tn

Acknowledgements

I would like to express my deepest gratitude to everyone who contributed to the successful completion of my internship. First and foremost, I sincerely thank **Arnox Engineering** for providing me with the invaluable opportunity to gain hands-on experience in the field of Mechanical Engineering.

I am especially grateful to **Mr. Ahmed BRAHAM**, my internship supervisor, for his continuous guidance, support, and insightful feedback throughout the internship. His expertise and encouragement have greatly deepened my understanding of both the subject matter and the professional environment.

Lastly, I would like to extend my appreciation to my academic institution, **Ecole Polytechnique de Tunisie**, for facilitating this internship and providing the necessary resources to make it possible. A heartfelt thank you to my professors and mentors for their unwavering academic guidance and encouragement throughout my studies.

Abstract

This report explores the modeling of elastomer materials under uniaxial stress using non-linear Finite Element Analysis (FEA). Elastomers have a unique, non-linear behavior when deformed, which makes accurate material modeling critical for engineering purposes. The aim of the study was to assess different hyperelastic models to identify the best one for capturing the stress-strain relationship in elastomers. Using MSC Marc software, simulations were run to replicate the material's behavior, and experimental data from uniaxial tests were used to fine-tune and validate these models. Several hyperelastic models, such as Neo-Hookean, Mooney-Rivlin, and Ogden, were evaluated, with the Ogden 3-term model standing out as the most precise in predicting how elastomers deform. These findings provide important guidance for choosing the right material models in engineering projects that involve elastomeric components.

Keywords: Elastomer modeling, Non-linear FEA, Hyperelastic models, Stress-strain relationship, MSC Marc, Ogden model, Uniaxial testing.

Contents

Acknowledgements	i
Abstract	ii
List of Figures	v
List of Tables	vi
1 General Context	1
1.1 Introduction	1
1.2 Presentation of the Host Company	1
1.3 Internship Scope	1
2 State of the Art	3
2.1 Introduction to MSC Marc	3
2.2 Understanding Non-Linear Finite Element Analysis (FEA)	4
2.2.1 Difference Between Linear and Nonlinear FEA	4
2.2.2 Types of Nonlinearity in FEA	5
2.2.3 Iterative Solution Methods in Nonlinear FEA	7
2.2.4 Incremental Loading	7
2.2.5 Convergence Criteria	7
2.3 Elastomeric Fitting	8
2.3.1 Hyperelastic Models	8
2.3.2 Curve Fitting Process	10
3 Elastomer Modeling and Fitting	12
3.1 Model Setup	12
3.1.1 Geometry	12
3.1.2 Boundary Conditions	12
3.1.3 Material Properties	13
3.1.4 Contact Surfaces	13
3.1.5 Loading Conditions	13
3.1.6 Simulation Configuration and Loadcase Setup	14
3.1.7 Visual Representation	15
3.2 Uniaxial Curve Fitting	16
3.2.1 Data Importation	16

3.2.2	Material Model Selection	16
3.3	Model Validation and Selection	21
3.3.1	RMSE Calculation	22
3.3.2	Visual Comparison of Models	22
3.3.3	Analysis of Results	24
3.4	Post-Processing: Stress and Strain Measures	24
4	Future Research and Conclusions	26
4.1	Future Research	26
4.2	Conclusions	26

List of Figures

2.1	Exemple of geometry nonlinearity : Analysis of a Rubber Seal	5
2.2	Exemple of Material nonlinearity : Super Plastic Forming of a Container	6
2.3	Exemple of Contact nonlinearity :Elastomeric Cylinder Seg to Seg Contact)	6
3.1	Fixed Displacement $x=0$	12
3.2	Fixed displacement $y=0$	12
3.3	Visualization of the rigid contact surfaces in the simulation	13
3.4	Force table applied to <code>cbody3</code>	14
3.5	Advanced Analysis Options in the simulation setup	14
3.6	Full compression of 50%	15
3.7	full extension of 200%	15
3.8	Stress versus Strain Plot	15
3.9	Uniaxial test data curve	16
3.10	Comparison of experimental uniaxial test data with the neo-Hookean model predictions	17
3.11	Comparison of experimental uniaxial test data with the Mooney-Rivlin (2-term) model predictions.	18
3.12	Comparison of experimental uniaxial test data with the Mooney-Rivlin (3-term) model predictions.	19
3.13	The Mooney-Rivlin (3-term) model predictions with positive coefficients .	19
3.14	Comparison of experimental uniaxial test data with the Ogden model predictions.	20
3.15	Ogden 2-term Coefficients	20
3.16	Ogden Control Parameters and Comparison of Experimental and Fitted Data	21
3.17	Visual Comparison of Models	23
3.18	Comparison of Engineering Strain versus Engineering Stress and Green-Lagrange Strain versus Cauchy Stress.	25

List of Tables

3.1	RMSE values for different hyperelastic models	22
-----	---	----

Chapter 1

General Context

1.1 Introduction

Finite Element Analysis (FEA) serves as a vital computational tool for simulating and analyzing complex structural behaviors under a variety of conditions. Non-linear FEA is particularly crucial for accurately modeling real-world scenarios where materials display non-linear characteristics such as plasticity or significant deformations. MSC Marc is a specialized software designed to perform these non-linear analyses with high precision. During my engineering internship at ArnoX Engineering, I focused on mastering non-linear FEA, beginning with an in-depth study of non-linearity principles. This foundation was then applied in hands-on projects, including the final project, which involved modeling an elastomer material under uniaxial stress to explore its deformation modes.

1.2 Presentation of the Host Company

ArnoX Engineering is an internationally recognized leader in the fields of CAD, CAM, CAE, PDM, and PLM training and consulting. The company has steadily grown, driven by its commitment to excellence and innovation. Specializing in advanced engineering solutions, ArnoX Engineering serves a diverse clientele, meeting various industry needs with precision and expertise. The growth of ArnoX has been entirely organic, reflecting their dedication to delivering top-tier services. Their team of elite professionals is globally recognized, placing ArnoX Engineering among the most prestigious training and consulting providers worldwide. Their approach is client-focused, ensuring that every solution is tailored to meet specific demands, contributing to their esteemed reputation in the engineering community[1].

1.3 Internship Scope

The scope of this internship was centered around developing a deep understanding of non-linear Finite Element Analysis (FEA) with a particular focus on modeling complex material behaviors. Throughout the internship, I studied various types of nonlinearity, including geometrical nonlinearity, boundary condition nonlinearity, and contact prob-

lems. These concepts are crucial in accurately simulating the behavior of materials under real-world conditions, where simple linear models are often insufficient.

In addition to the theoretical study, I performed several simulations using MSC Marc, applying the knowledge gained about nonlinearity to model an elastomer material under uniaxial stress. The simulations involved defining appropriate boundary conditions, handling material non-linearities, and addressing contact problems between different bodies. The primary objective was to explore how these nonlinear factors influence the material's stress-strain response, providing insights that are essential for advanced engineering applications.

Chapter 2

State of the Art

Introduction

The second chapter explores non-linear Finite Element Analysis (FEA) using MSC Marc software, discussing linear and non-linearity types, iterative solution methods, hyperelastic models, and elastomeric modeling curve-fitting processes, including the Newton-Raphson method.

2.1 Introduction to MSC Marc

MSC Marc is a leading software solution for non-linear Finite Element Analysis (FEA), widely recognized for its ability to handle complex simulations that involve large deformations, material nonlinearity, and intricate contact conditions. Developed by MSC Software, Marc is specifically designed to address the challenges posed by non-linear problems in engineering, where traditional linear FEA methods may fall short.

The software provides a robust platform for simulating real-world physical behaviors in a variety of materials, including metals, plastics, and elastomers. Marc's advanced capabilities include the simulation of static and dynamic events, thermal analysis, and coupled multiphysics problems. It is particularly effective in industries such as automotive, aerospace, and biomechanics, where precision in modeling non-linear behavior is crucial.

Key features of MSC Marc include:

- **Advanced Material Models:** Supports a wide range of material models, including elastic, plastic, viscoelastic, and hyperelastic models.
- **Large Deformation Analysis:** Accurately models scenarios where structures undergo significant changes in shape.
- **Contact Analysis:** Efficiently handles complex contact interactions between multiple bodies, including frictional and adhesive contacts.
- **Coupled Multiphysics:** Allows for the integration of thermal, structural, and fluid dynamics within a single analysis.

MSC Marc's user-friendly interface, combined with its powerful simulation capabilities, makes it an essential tool for engineers and researchers dealing with non-linear problems.

2.2 Understanding Non-Linear Finite Element Analysis (FEA)

Nonlinear Finite Element Analysis (FEA) is an advanced computational technique used to solve complex engineering problems where linear assumptions no longer hold true. Unlike linear FEA, which assumes a proportional relationship between applied loads and displacements, nonlinear FEA accounts for nonlinearities in material behavior, geometry, or boundary conditions. Nonlinear analysis is crucial in accurately predicting the behavior of structures under large deformations, complex loadings, or when the material properties change significantly during loading.

2.2.1 Difference Between Linear and Nonlinear FEA

Linear FEA is based on the assumption that:

- The relationship between the applied forces (load) and the resulting displacements is linear (i.e., they are directly proportional).
- Material properties remain constant during deformation.
- Deformations are small, so the initial geometry of the system does not change significantly.

The governing equation for linear FEA is:

$$Ku = F$$

where:

- K is the global stiffness matrix,
- u is the displacement vector,
- F is the load vector.

In linear FEA, the stiffness matrix K is constant, and the system of equations is solved in one step.

Nonlinear FEA, on the other hand, deals with situations where:

- The relationship between forces and displacements is nonlinear.
- The material properties may vary as the structure deforms (material nonlinearity).
- Large deformations may change the geometry significantly (geometric nonlinearity).
- Boundary conditions may also change during the loading process (boundary condition nonlinearity).

The general equation for nonlinear FEA is an iterative form:

$$K(u)\Delta u = \Delta F$$

where:

- $K(u)$ is the stiffness matrix, which now depends on the displacement u ,
- Δu is the incremental change in displacement,
- ΔF is the incremental load.

In nonlinear FEA, the stiffness matrix changes as the system deforms, making it necessary to use iterative methods like the Newton-Raphson method to solve the problem.

2.2.2 Types of Nonlinearity in FEA

• Geometric Nonlinearity

Geometric nonlinearity arises when the deformations are large enough to affect the system's geometry, making the stiffness matrix a function of the current displacement configuration. This type of nonlinearity is common in problems involving large deformations, such as in buckling, post-buckling, or large deflection analysis of structures.

The governing equation for geometric nonlinearity is derived from the updated configuration, not the initial one:

$$K(u)u = F$$

where $K(u)$ now depends on the updated geometry of the structure.

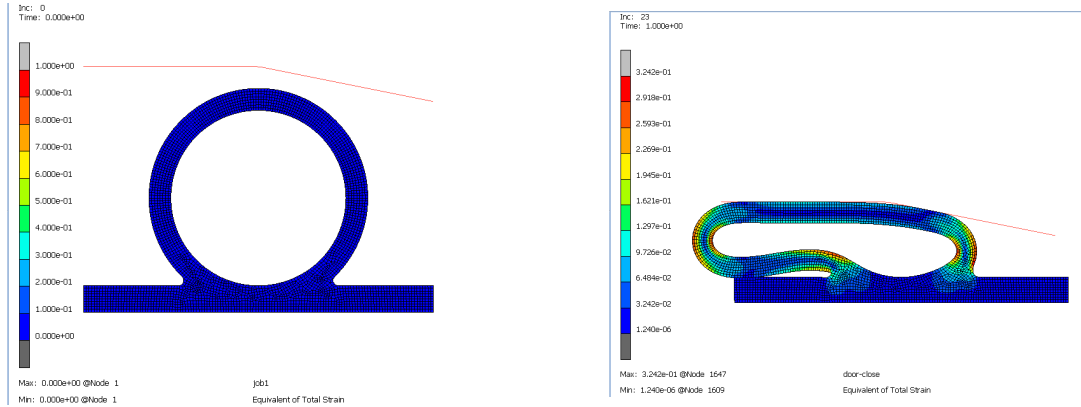


Figure 2.1: Exemple of geometry nonlinearity : Analysis of a Rubber Seal

• Material Nonlinearity

Material nonlinearity occurs when the material behavior deviates from linear elasticity, such as in plasticity, hyperelasticity, viscoelasticity, or damage models. In this case, the stress-strain relationship is nonlinear, meaning the stress is not directly proportional to the strain. For example, in plasticity, the material deforms plastically after reaching the yield stress, and any further loading causes permanent deformation.

The nonlinear stress-strain relationship can be expressed as:

$$\sigma = f(\epsilon)$$

In the case of plasticity, the material obeys a constitutive law such as:

$$\sigma = E\epsilon \quad (\text{for elastic behavior}), \quad \sigma = \sigma_y + H(\epsilon_p) \quad (\text{for plastic behavior})$$

where σ_y is the yield stress, and $H(\epsilon_p)$ is the hardening function that describes how the material continues to harden with plastic strain ϵ_p .

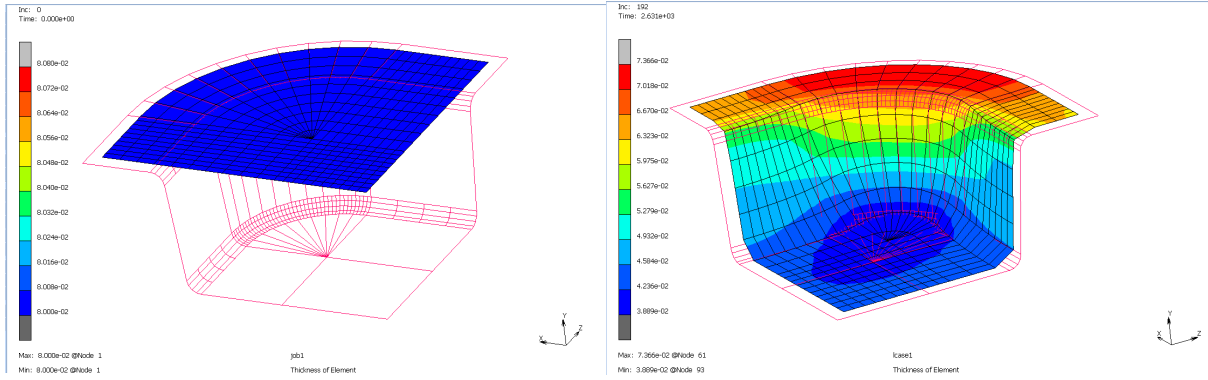


Figure 2.2: Exemple of Material nonlinearity : Super Plastic Forming of a Container

• Boundary Condition (Contact) Nonlinearity

Boundary condition nonlinearity arises when there are changes in the boundary conditions during the analysis, such as when contact or separation between two or more bodies occurs. For example, in contact problems, surfaces that are initially not in contact may come into contact during loading, introducing nonlinearity. This requires special contact algorithms to handle conditions like friction or sliding.

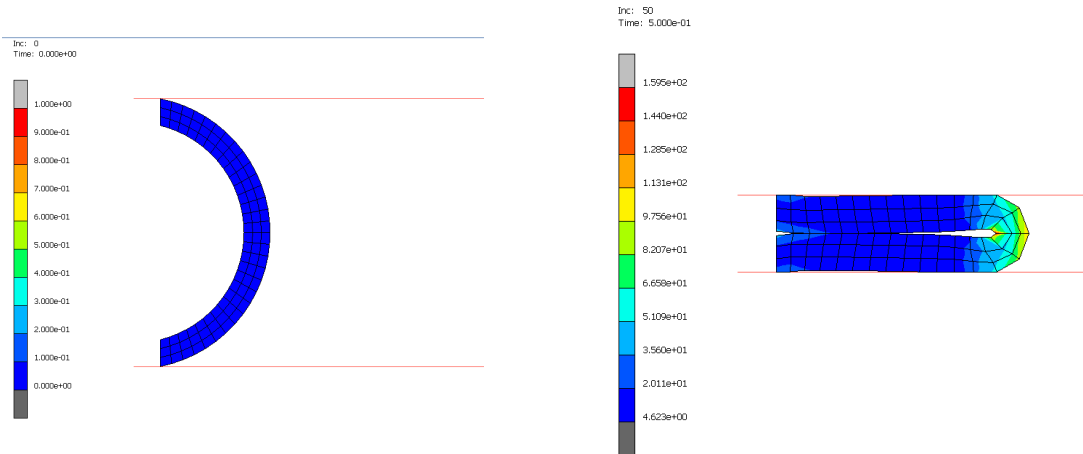


Figure 2.3: Exemple of Contact nonlinearity :Elastomeric Cylinder Seg to Seg Contact)

2.2.3 Iterative Solution Methods in Nonlinear FEA

Since nonlinear problems are inherently more complex, they are typically solved using iterative techniques. The most common method is the **Newton-Raphson method**, which is used to iteratively solve the nonlinear equation:

$$K(u^n)\Delta u^n = R(u^n)$$

where:

- u^n is the current estimate of displacement at iteration n ,
- Δu^n is the incremental change in displacement at iteration n ,
- $R(u^n)$ is the residual, i.e., the difference between the applied and internal forces.

The Newton-Raphson method updates the solution vector \mathbf{D} iteratively as:

$$\mathbf{D}^{(i+1)} = \mathbf{D}^{(i)} - \mathbf{K}^{-1}(\mathbf{D}^{(i)})\mathbf{R}(\mathbf{D}^{(i)})$$

where:

- \mathbf{D} is the displacement vector.
- $\mathbf{K}(\mathbf{D})$ is the tangent stiffness matrix.
- $\mathbf{R}(\mathbf{D})$ is the residual force vector.

The Newton-Raphson method improves convergence by iteratively updating the stiffness matrix and displacement values until the residual is minimized.

2.2.4 Incremental Loading

In non-linear FEA, loads are applied incrementally in steps, and the solution is obtained iteratively at each step.

The choice of load increments $\Delta\lambda_n$ is crucial and depends on the nature of the equilibrium path:

$$\Delta\lambda_{n+1} = \Delta\lambda_n \cdot \left(\frac{N_{\text{desired}}}{N_n} \right)$$

where N_{desired} is the desired number of iterations for convergence, and N_n is the actual number of iterations required in step n .

2.2.5 Convergence Criteria

Convergence criteria are used to check if the iterative solution is converging to the correct answer. These criteria are essential for ensuring that the solution meets the necessary accuracy without excessive computational effort. Common convergence criteria include:

- **Displacement Convergence:** Measures the change in displacements between iterations.
- **Force Convergence:** Checks the balance between internal and external forces.
- **Energy Convergence:** Ensures that the energy balance is satisfied, based on the product of residual forces and displacements.

2.3 Elastomeric Fitting

Elastomeric materials, such as rubber, exhibit highly non-linear stress-strain behavior due to their capability to undergo large elastic deformations. Accurate modeling of these materials requires specialized hyperelastic models rather than traditional linear elastic models. The primary challenge lies in fitting these models to experimental data obtained from various deformation tests.

2.3.1 Hyperelastic Models

The basis for any hyperelastic-material model is the strain energy density function W . In the general case of an anisotropic hyperelastic solid, the strain energy density function must be a symmetrical function of the stretch ratios λ_1 , λ_2 , and λ_3 . Therefore, W can be defined with three invariants I_1 , I_2 , I_3 :

$$\begin{aligned} I_1 &= \lambda_1^2 + \lambda_2^2 + \lambda_3^2 \\ I_2 &= \lambda_1^2 \lambda_2^2 + \lambda_2^2 \lambda_3^2 + \lambda_1^2 \lambda_3^2 \\ I_3 &= \lambda_1^2 \lambda_2^2 \lambda_3^2 \end{aligned}$$

Thus,

$$W = f(\lambda_1, \lambda_2, \lambda_3)$$

In hyperelastic-material research, various models are used to define the strain energy function.

Generalized Mooney-Rivlin Model

The Generalized Mooney-Rivlin model is a polynomial function of the strain energy density that provides a better fit with test data for both unfilled and filled rubbers. It is expressed as:

$$W = \sum_{i,j=1}^N C_{ij} (I_1 - 3)^i (I_2 - 3)^j + \sum_{i=1}^N \frac{1}{D_i} (I_3 - 1)^{2i}$$

where:

- W is the strain energy potential.
- I_1, I_2 are strain invariants, measures of distortion in the material.
- I_3 is the elastic volume ratio or third strain invariant.
- C_{ij} is related to the shear behavior of the material.
- D_i characterizes the compressibility of the material.
- N is the order of the polynomial.

For fully incompressible materials ($I_3 = 1$), the second part of the equation becomes null.

Mooney-Rivlin Model

The Mooney-Rivlin model is a special case of the Generalized Mooney-Rivlin model and is commonly used to describe the behavior of vulcanized rubber under simple tension. It is given by:

$$W = C_{10}(I_1 - 3) + C_{01}(I_2 - 3) + C_{11}(I_1 - 3)(I_2 - 3)$$

where C_{10}, C_{01}, C_{11} are material constants.

Yeoh Model

The Yeoh model differs from other higher-order polynomial models as it depends only on the first strain invariant:

$$W = C_{10}(I_1 - 3) + C_{20}(I_1 - 3)^2 + C_{30}(I_1 - 3)^3$$

This model is particularly useful as it fits various deformation modes using data obtained from uniaxial tension tests only, reducing the need for extensive material testing.

Arruda-Boyce Model

The Arruda-Boyce model is based on statistical mechanics and derived from an eight-chain network model. The strain energy function is given by:

$$W = nKT \left[(I_1 - 3) + \frac{1}{5}(I_1 - 3)^2 + \frac{1}{105}(I_1 - 3)^3 + \frac{1}{519}(I_1 - 3)^4 + \dots \right]$$

where:

- n is the chain density.
- K is the Boltzmann constant.
- T is the temperature.
- I_1 is the first invariant of the left Cauchy-Green deformation tensor.

Ogden Model

The Ogden model expresses the strain energy density as a sum of terms involving powers of the principal stretches:

$$W = \sum_{k=1}^N a_k (\lambda_1^{\alpha_k} + \lambda_2^{\alpha_k} + \lambda_3^{\alpha_k} - 3)$$

where:

- N is the number of terms in the series.
- a_k and α_k are material constants.
- $\lambda_1, \lambda_2, \lambda_3$ are the principal stretches.

For incompressible materials, the constraint $J = \lambda_1 \lambda_2 \lambda_3 = 1$ holds.

2.3.2 Curve Fitting Process

The process of elastomeric fitting involves calibrating these hyperelastic models to match experimental data obtained from material tests. The typical steps in the curve fitting process include:

Data Collection

The determination of property constants for rubber materials is challenging, as these constants are less readily available in the literature compared to those for typical engineering materials such as steel, aluminum, and titanium. Often, this data is only obtainable through specialized testing methods.

Multiple types of experimental data are required to fully characterize elastomeric materials. These tests include:

- Simple Tension Test
- Planar Tension Test
- Equibiaxial Extension Test
- Shear Test
- Volumetric Test

The process of material test data curve fitting is essential in determining the elastomeric material constants. This process depends significantly on the deformation state, specimen geometry, and the specific measurements taken. The two major modes of deformation that are typically analyzed are:

Uniaxial Tension: Where the material is stretched in one direction, resulting in a simple elongation.

Equibiaxial Tension: Where the material is stretched equally in two directions, often used as an equivalent to uniaxial compression.

Model Selection

A suitable hyperelastic model is selected based on the material behavior and the type of deformation expected in the application. For instance, the Neo-Hookean model might be used for simple applications with small deformations, while the Ogden model might be necessary for more complex scenarios.

Parameter Estimation

The material parameters (e.g., $C_{10}, C_{01}, C_{11}, J_m, a_k, \alpha_k$) in the selected model are estimated by fitting the model to the experimental data. This is typically done using a least-squares optimization technique that minimizes the difference between the model predictions and the experimental data:

$$\text{Minimize } \sum_{i=1}^n (\sigma_{\text{model}}(i) - \sigma_{\text{exp}}(i))^2$$

where:

- $\sigma_{\text{model}}(i)$ is the stress predicted by the hyperelastic model.
- $\sigma_{\text{exp}}(i)$ is the experimentally measured stress.

Conclusion

The MSC Marc software and non-linear FEA principles provide a theoretical foundation for material simulations, clarifying concepts like linear and non-linearities, hyperelastic models, and their practical relevance in analyzing elastomer deformation behavior.

Chapter 3

Elastomer Modeling and Fitting

Introduction

This chapter discusses elastomer modeling using non-linear FEA, covering geometry, boundary conditions, material properties, contact surfaces, loading conditions, simulations, and hyperelastic models like Neo-Hookean and Mooney-Rivlin..

3.1 Model Setup

3.1.1 Geometry

The uniaxial stress analysis employs a single cubic element to represent a homogeneous elastomeric material, enabling a thorough examination of the stress-strain relationship under uniaxial loading..

The cube is modeled with equal sides in all three dimensions (X, Y, Z), $a = 1\text{mm}$, which simplifies the analysis and ensures uniform stress distribution when subjected to uniaxial stress.

3.1.2 Boundary Conditions

Boundary conditions dictate cube element interaction with forces and environment. Constrained faces on $x=0$ and $y=0$ planes prevent free translation, ensuring element remains fixed.

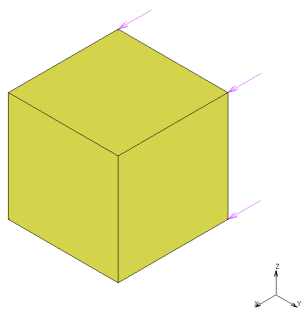


Figure 3.1: Fixed Displacement $x=0$

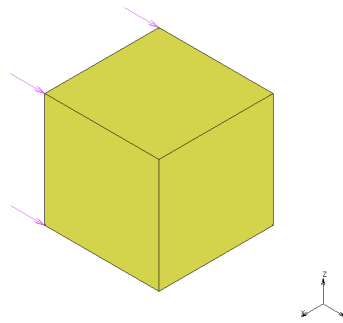


Figure 3.2: Fixed displacement $y=0$

3.1.3 Material Properties

The material used in this simulation is an elastomeric material, represented by the neo-Hookean hyperelastic model. The key material properties defined in the model setup are:

- **Material Model:** Neo-Hookean Hyperelastic Model
- **Material Constant (C_{10}):** $C_{10} = 0.5$

This constant is a crucial parameter in the neo-Hookean model, representing the material's shear modulus, which directly influences its stress-strain response under deformation.

The neo-Hookean model will be used for simulation, followed by more complex hyperelastic models like Mooney-Rivlin and Ogden to evaluate material response under different loading conditions.

3.1.4 Contact Surfaces

The deformation is imposed using rigid contact surfaces. The lower rigid body (`cbody2`) is stationary, while the upper rigid body (`cbody3`) is moved to first push and then pull the cubic element.

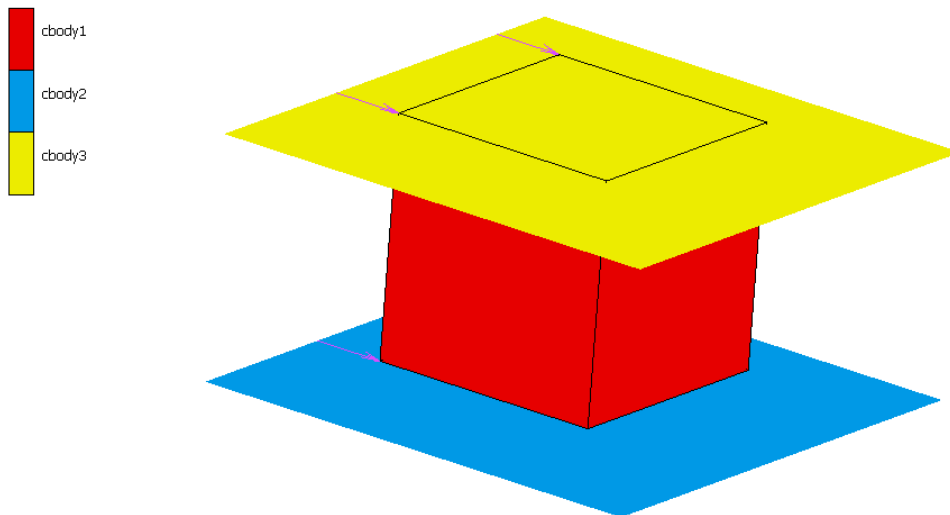


Figure 3.3: Visualization of the rigid contact surfaces in the simulation

3.1.5 Loading Conditions

The loading is applied in 40 equal time increments:

- **Increment 10:** The cubic element is fully compressed to 50% of its original height.

- **Increment 30:** The cube is extended to 200% of its original height, representing full extension.
- **Increment 40:** The cube returns to its original configuration, completing the loading cycle.

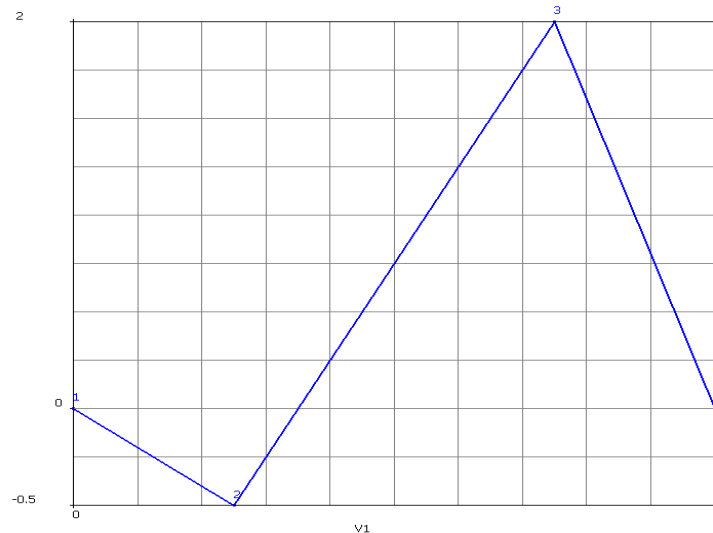


Figure 3.4: Force table applied to `cbody3`

The plot shows the variation of force over time, which is introduced to the upper rigid body (`cbody3`) to simulate the compression and decompression cycle on the cubic element. The force increments correspond to the different stages of the loading condition, with the maximum force applied at Increment 30 to achieve full extension of the element.

3.1.6 Simulation Configuration and Loadcase Setup

The simulation's loadcase properties were configured with a total loadcase time of 1 unit, utilizing a constant time step of 0.025 over 40 steps. Fixed time stepping was employed, with automatic time step cut back enabled to allow up to 10 cut backs, ensuring stability throughout the process.

The Total Lagrange formulation was used to handle large strains. These configurations were critical in accurately simulating the material behavior under uniaxial stress.

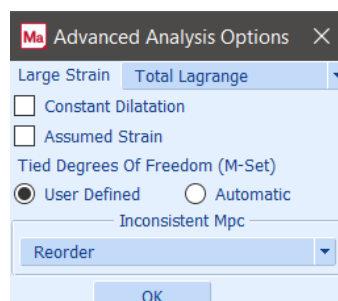


Figure 3.5: Advanced Analysis Options in the simulation setup

3.1.7 Visual Representation

Now, let's look at the results of this analysis before curve fitting our uniaxial test data.

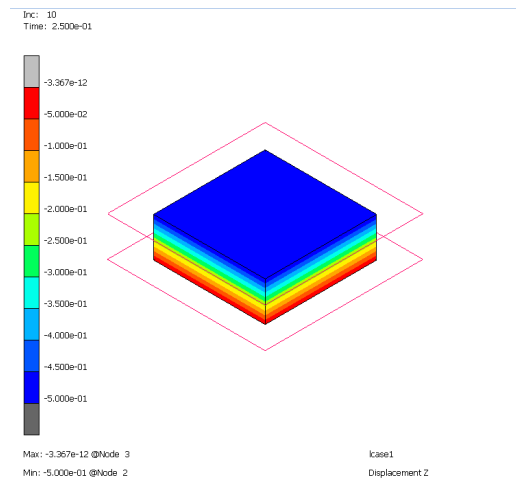


Figure 3.6: Full compression of 50%

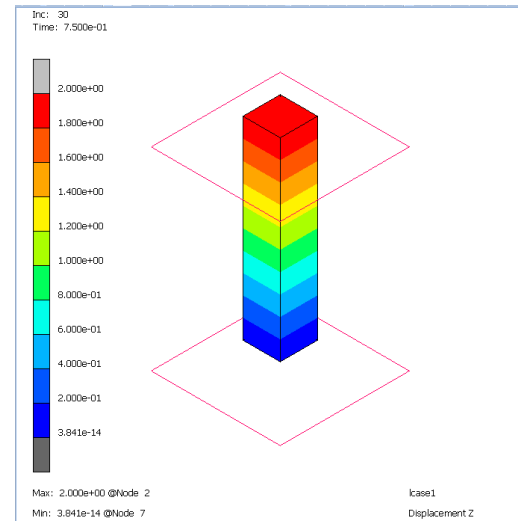


Figure 3.7: full extension of 200%

Now let's generate the stress-strain plot that the Marc analysis has calculated.

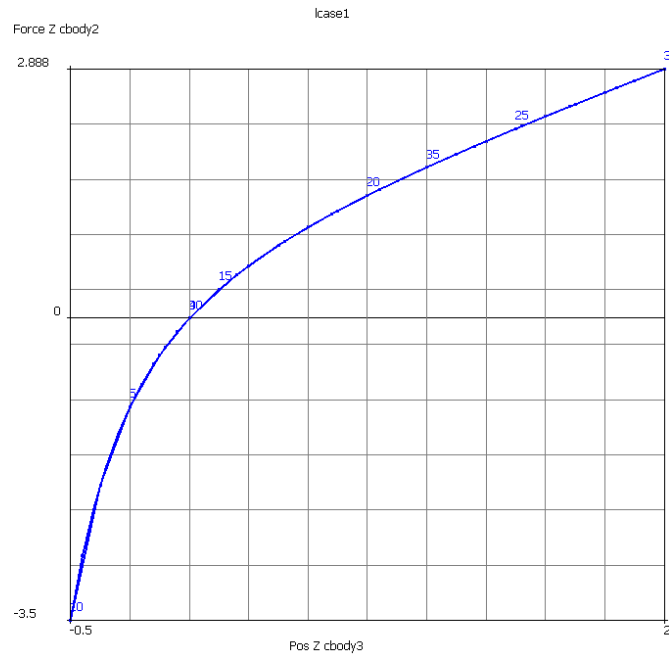


Figure 3.8: Stress versus Strain Plot

Since the original area is one, and since the original length in the z-direction is one, the above plot is the engineering stress versus the engineering strain for a uniaxial stress specimen with neo-Hookean behavior. We use the Body 2 force just to get the sign correct.

3.2 Uniaxial Curve Fitting

Using the created model file, we will redefine the material by reading the uniaxial data, and proceed to re-run the problem using neo-Hookean, Mooney 2-term, Mooney 3-term, and Ogden 2-term fits.

3.2.1 Data Importation

The data importation process involves loading uniaxial test data into the simulation software for curve fitting. This is done by reading the test data file provided by the experimental testing of the material. The file is imported into the software, enabling the data to be used for defining material properties in the subsequent analysis.

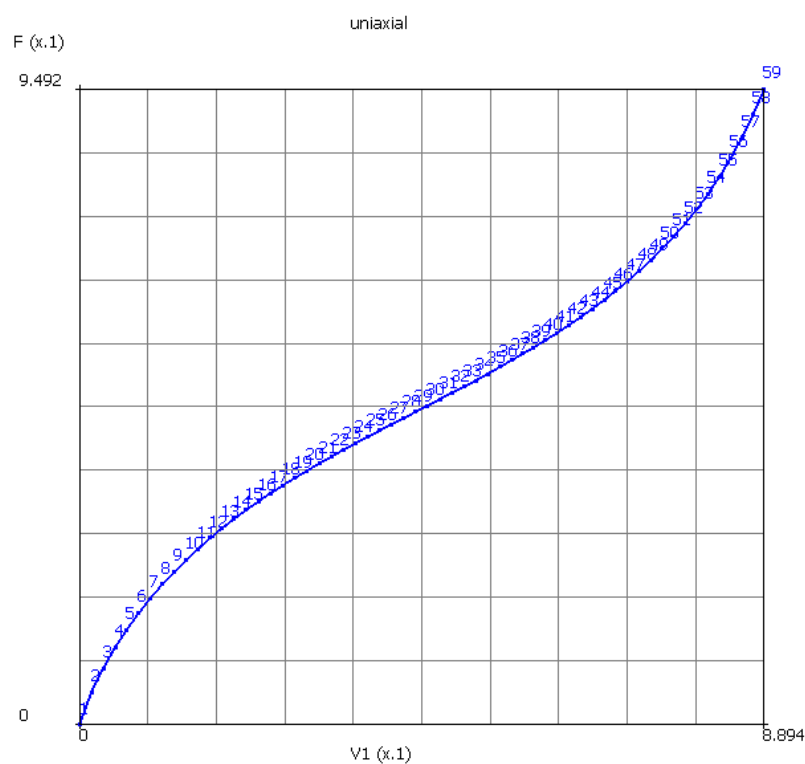


Figure 3.9: Uniaxial test data curve

The curve represents the material's response under uniaxial tension, which will be used for fitting various hyperelastic material models to accurately capture the material's behavior.

3.2.2 Material Model Selection

Once the test data is loaded, redefine the material properties using this experimental data. The fitting process involves running the analysis using various hyperelastic models:

• Neo Hookean

For the curve fitting process, the neo-Hookean model is selected. The curve fitting routine is based solely on the uniaxial test data. By using the **COMPUTE** button, the software calculates the model coefficients. For the neo-Hookean model, the single coefficient C_{10} is determined to be 0.265. The responses for multiple modes are plotted by default, allowing for a comprehensive evaluation of the fit quality.

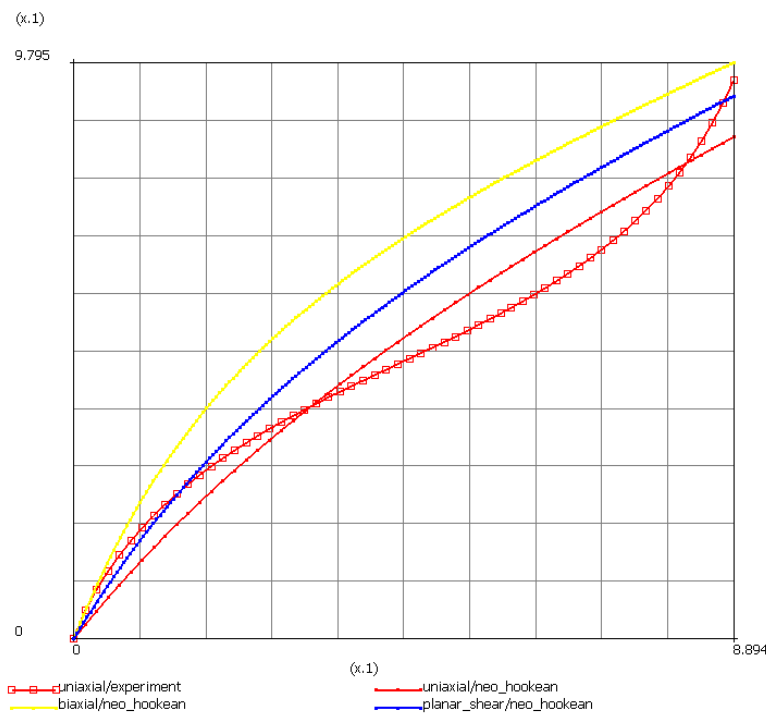


Figure 3.10: Comparison of experimental uniaxial test data with the neo-Hookean model predictions

We have just fit a neo-Hookean model using only uniaxial data. Mentat, by default, shows the model's response in all major modes of deformation.

If we Look again at the previous stress-strain plot. The Uniaxial is the lowest magnitude, the planar shear is higher, and the biaxial response is the highest. This is typical of most elastomer.

We initially used the neo-Hookean model for curve fitting because it is a simple model that is often sufficient for capturing the general curvature of the test data. As a best practice, it is recommended to start with simpler models when fitting material data. If the simple model adequately captures the behavior of the material, it can be used for further analysis. Only if the simple model fails to represent the material behavior accurately should more complex, higher-order models be considered.

- **Mooney-Rivlin 2-term**

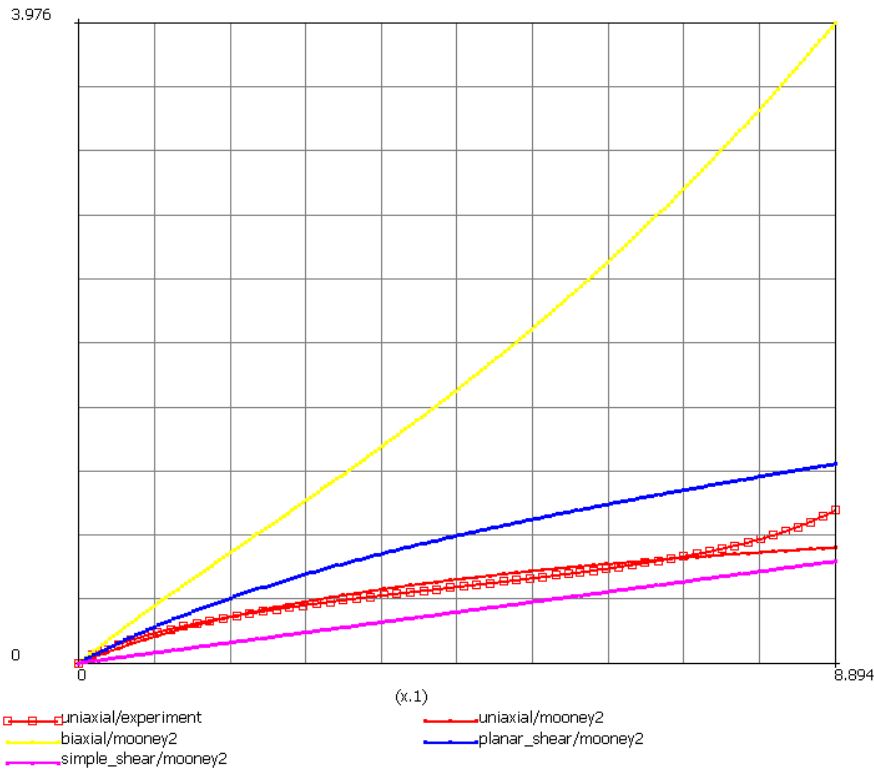


Figure 3.11: Comparison of experimental uniaxial test data with the Mooney-Rivlin (2-term) model predictions.

we fit a Mooney-Rivlin 2-term material model to the data. The Mooney-Rivlin coefficients obtained are $C_{10} = 0.074$ and $C_{01} = 0.280$. The positive values of these coefficients guarantee the stability of the model. The biaxial stiffness is approximately four times higher than that of the earlier material model. As expected, the fit to the uniaxial data is improved with the Mooney-Rivlin model, which is capable of capturing more curvature in the stress-strain data due to the additional term.

- **Mooney-Rivlin 3-term**

The obtained Mooney-Rivlin coefficients are $C_{10} = -0.735$, $C_{01} = 1.21$, and $C_{11} = 0.194$. The uniaxial response from this model is exceptional; however, the presence of a negative coefficient indicates that the material model might be unstable. This potential instability requires a visual examination to determine the stability range of the model. It is also noteworthy that the peak stress for the biaxial response has increased significantly across the models: from 1.0 (neo-Hookean), to 4.5 (Mooney 2-term), and now to 36 (Mooney 3-term). The question remains: which model provides the correct prediction?

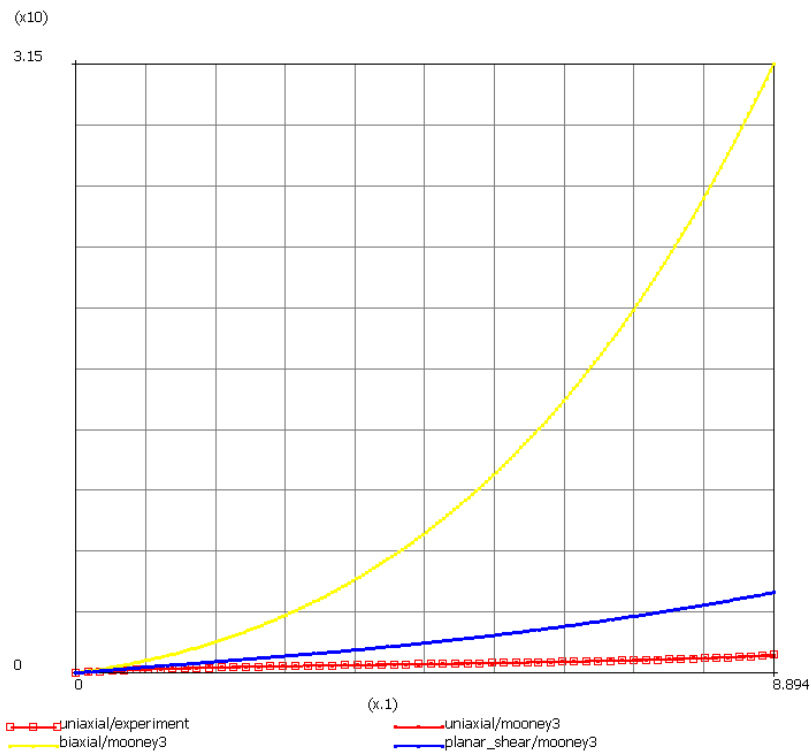


Figure 3.12: Comparison of experimental uniaxial test data with the Mooney-Rivlin (3-term) model predictions.

Now we will try to fit the model with the Positive coefficients option to see how much the responses change.

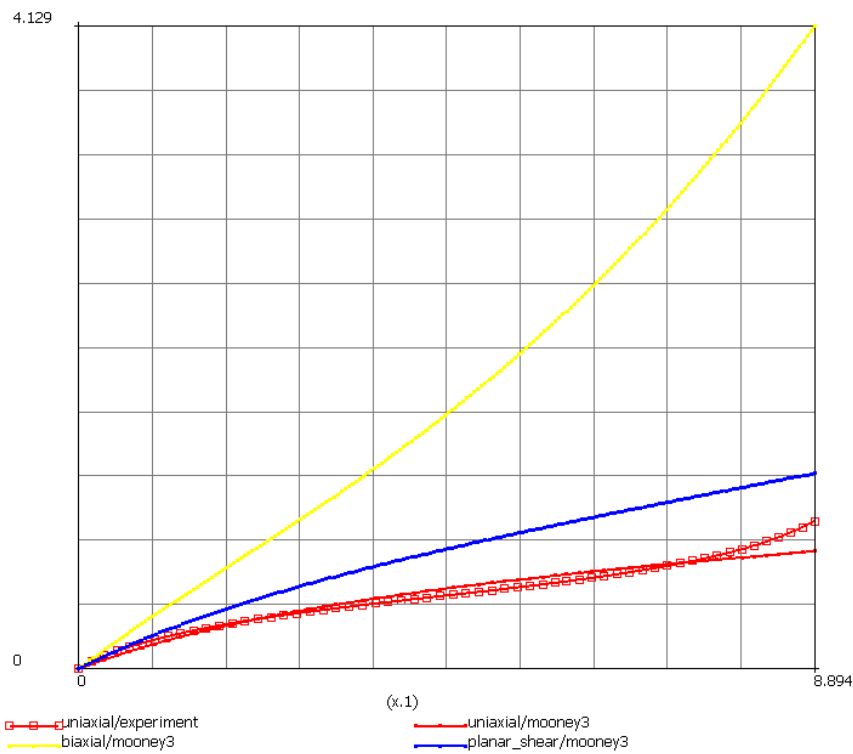


Figure 3.13: The Mooney-Rivlin (3-term) model predictions with positive coefficients

- Ogden 2-term

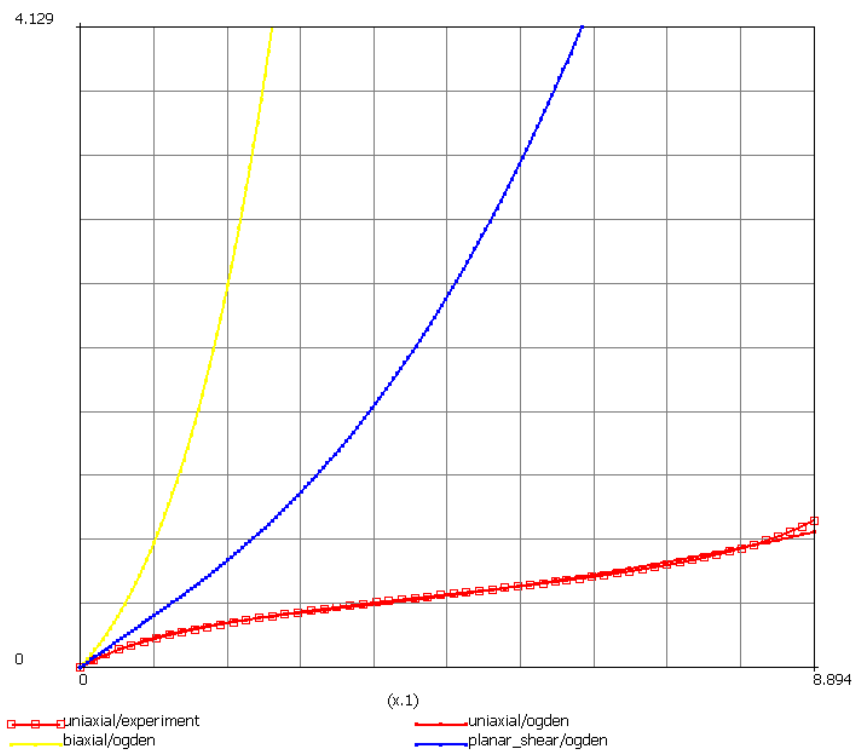


Figure 3.14: Comparison of experimental uniaxial test data with the Ogden model predictions.

Now, an Ogden 2-term material model is fitted to the data. The uniaxial response is very good, but the biaxial response is now even higher than that of the Mooney 3-term model. Ogden coefficients come in pairs, where the moduli are denoted by μ_i and the exponents by α_i . Stability is guaranteed if each μ_i and α_i have the same sign. However, if a μ_i is positive and its corresponding α_i is negative (or vice versa), the material model might be unstable. Therefore, a visual determination of the stability range of the model is necessary.

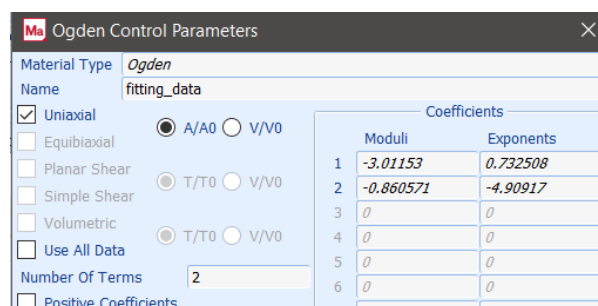


Figure 3.15: Ogden 2-term Coefficients

• Ogden 3-term

Now we fit the Ogden 3-terms model:

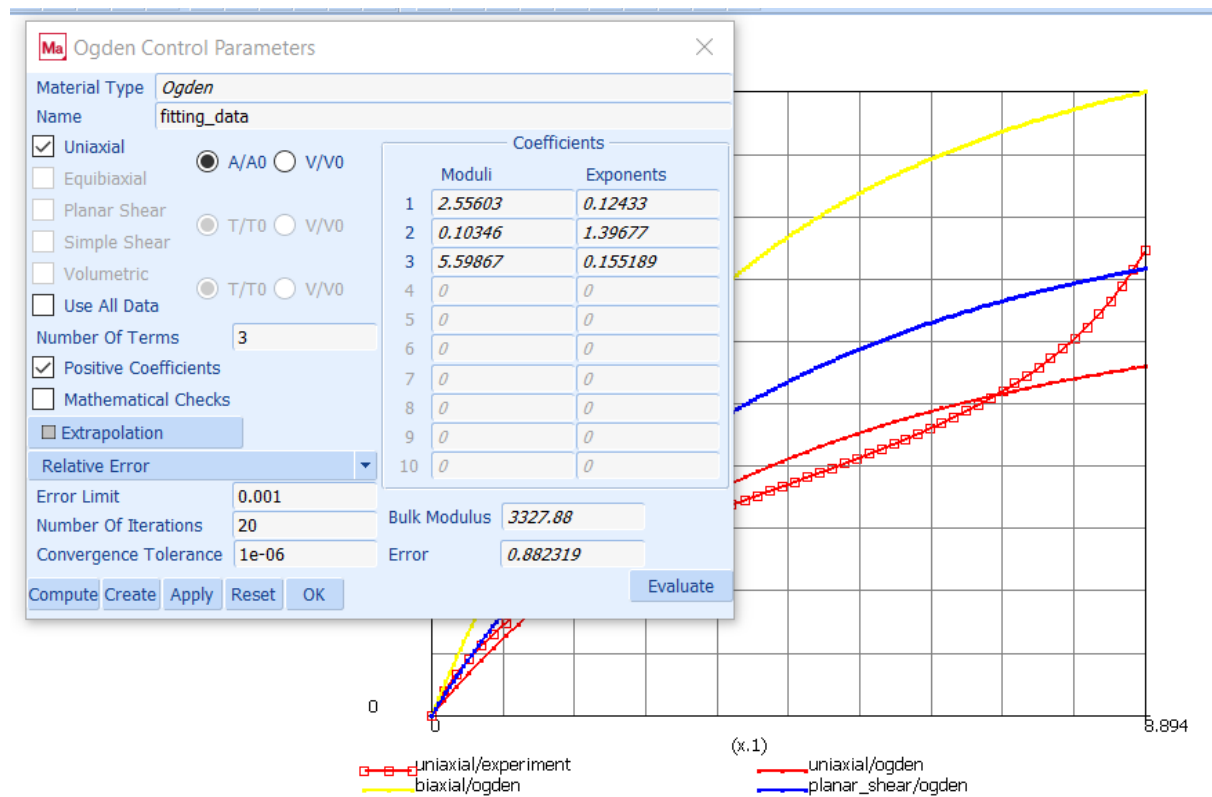


Figure 3.16: Ogden Control Parameters and Comparison of Experimental and Fitted Data

The computed coefficients for the moduli and exponents are displayed in the image, alongside the stress-strain plots comparing the Ogden model predictions with the experimental data.

The Ogden model with three terms provided a good fit to the experimental uniaxial data, as evidenced by the close alignment of the model's predictions with the experimental curve (red line). The planar shear and equibiaxial predictions (blue and yellow lines) are also displayed, showing the model's capability in predicting different deformation modes. The bulk modulus and overall error values indicate a reasonable level of accuracy for the model.

3.3 Model Validation and Selection

The validation of the material models used to simulate the elastomer under uniaxial stress was primarily based on comparing the root mean square error (RMSE) between the experimental data and the predictions of each model. This section discusses the methodology used for this validation, the results obtained, and the selection of the most appropriate model based on these results.

3.3.1 RMSE Calculation

RMSE values were calculated for each material model to quantify the differences between the experimental data and the simulated results.

The RMSE formula used on for comparison involved experimental and predicted stress values, here's the tailored equation:

$$\text{RMSE} = \sqrt{\frac{1}{N} \sum_{i=1}^N (\sigma_{\text{exp},i} - \sigma_{\text{model},i})^2} \quad (3.1)$$

The models evaluated include Neo-Hookean, Mooney-Rivlin 2-term, Mooney-Rivlin 3-term, Ogden 2-term, and Ogden 3-term. The RMSE for each model is presented in Table 3.1.

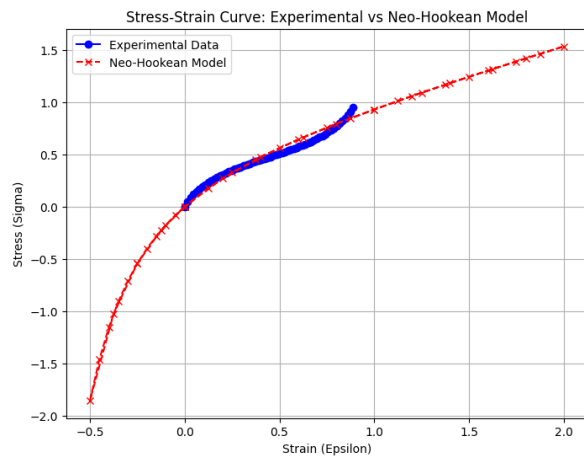
Model	RMSE
Neo-Hookean	0.771
Mooney-Rivlin 2-term	1.203
Mooney-Rivlin 3-term	1.174
Ogden 2-term	0.855
Ogden 3-term	0.851

Table 3.1: RMSE values for different hyperelastic models

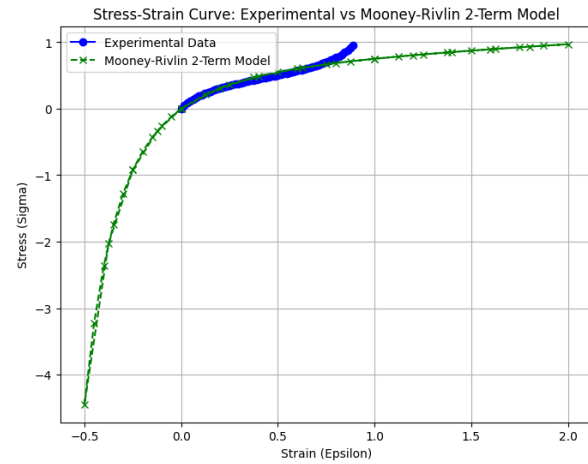
3.3.2 Visual Comparison of Models

Each material model was implemented in MSC Marc to simulate the uniaxial stress response of the elastomer. Simulations were conducted separately for each model, ensuring that the boundary conditions, loading sequences, and other simulation parameters were consistently applied across all models to maintain the validity of the comparison.

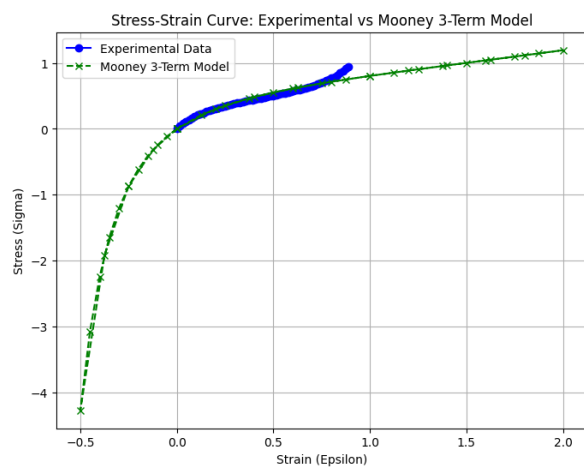
The stress-strain curves for the experimental data and each model's predictions were plotted using python to visually assess the fit. The curves demonstrate how each model captures the behavior of the material under uniaxial loading conditions.



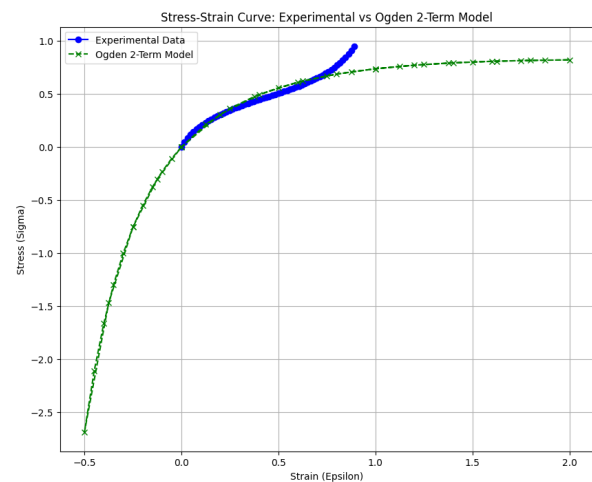
(a) Stress-Strain comparison for the Neo-Hookean model.



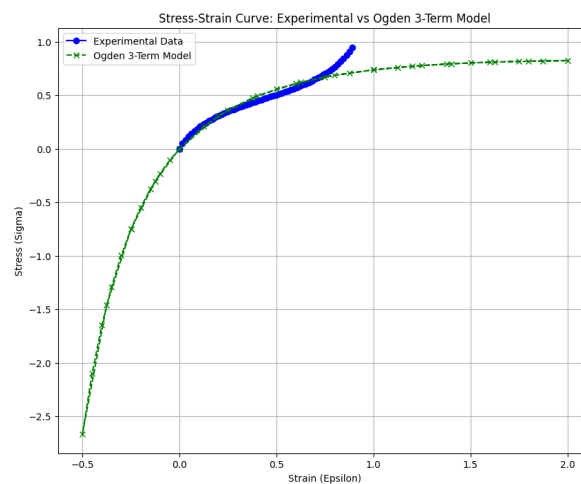
(b) Stress-Strain comparison for the Mooney-Rivlin 2-term model.



(c) Stress-Strain comparison for the Mooney-Rivlin 3-term model.



(d) Stress-Strain comparison for the Ogden 2-term model.



(e) Stress-Strain comparison for the Ogden 3-term model.

Figure 3.17: Visual Comparison of Models

3.3.3 Analysis of Results

The Ogden 3-term model was chosen for a project due to its precision and visual agreement with experimental data. The model had the lowest RMSE values and demonstrated a high level of accuracy in predictions. It excelled across all tested strains, reproducing the complex behavior of elastomeric materials under diverse conditions. This fidelity is crucial for applications requiring detailed and precise material characterization. The model's robustness was confirmed through rigorous simulations, making it a reliable tool for predicting material responses under varied loading scenarios. This makes the Ogden 3-term model an invaluable asset for engineers and designers requiring detailed material analysis to ensure product safety and functionality.

3.4 Post-Processing: Stress and Strain Measures

In order to plot the engineering stress and strain measures to conduct the comparison previously done, we plotted “Pos Z cbody3” versus “Force Z cbody2” and because the original length and cross-sectional area are unity, “Pos Z cbody3” versus “Force Z cbody2” is the engineering strain versus the engineering stress.

Since a total Lagrangian formulation is being used, the stress and strain measures (or Lagrangian measures) on the post file are Cauchy stress and Green-Lagrange strain which are different than the engineering measures. In this section, we shall convert the Lagrangian measures to engineering measures.

Conversion of Lagrangian Measures to Engineering Measures

After obtaining the simulation results in terms of Green-Lagrange strain and Cauchy stress, it is necessary to convert these measures into their engineering equivalents for a more intuitive understanding and comparison with experimental data.

Mathematical Relations for Conversion

For this specific uniaxial problem, where the direction of deformation is along the z-axis, the engineering strain (ϵ_{33}) and stress (σ_{33}) are related to the Green-Lagrange strain (E_{33}) and the Cauchy stress (t_{33}) as follows:

$$\epsilon_{33} = \sqrt{2E_{33} + 1} - 1 \quad (3.2)$$

$$\sigma_{33} = \frac{t_{33}}{1 + \epsilon_{33}} \quad (3.3)$$

These formulas are derived from the definition of Green-Lagrange strain, where:

$$E_{ij} = \frac{1}{2} ([F]^T [F] - \delta_{ij}) \quad (3.4)$$

Here, $[F]$ represents the deformation gradient determined from the stretch ratios. Given the assumption of incompressibility, the following relationship holds:

$$\sigma_{33} = \frac{t_{33}}{\lambda} = \frac{t_{33}}{1 + \epsilon_{33}} \quad (3.5)$$

These conversions allow us to represent the simulation data in the standard engineering format, which is more familiar and easier to interpret. By applying these equations, the stress-strain data obtained from the Ogden model analysis can be directly compared to experimental results, thereby validating the accuracy of the simulation.

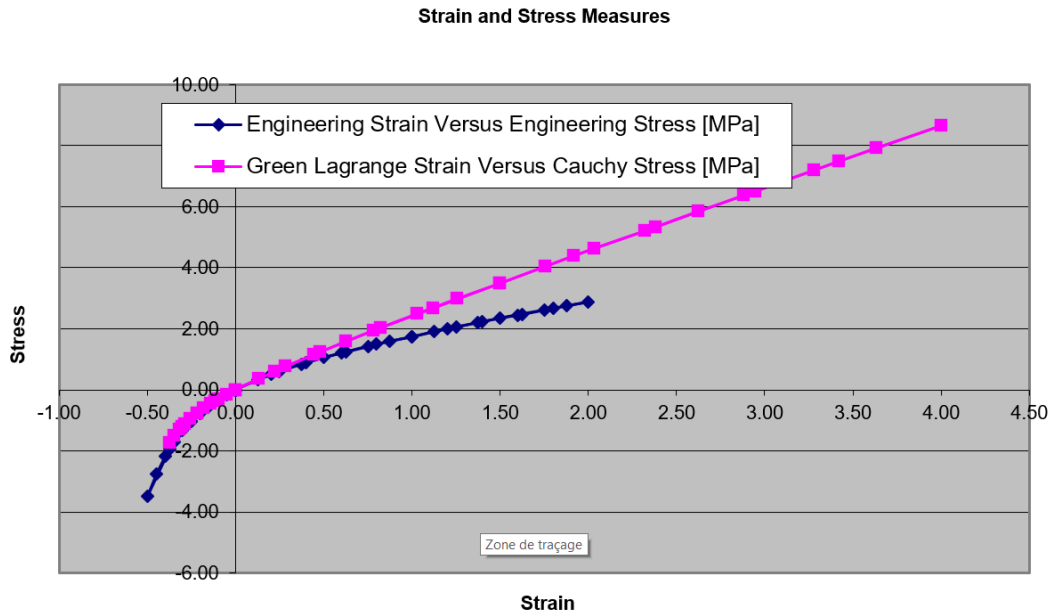


Figure 3.18: Comparison of Engineering Strain versus Engineering Stress and Green-Lagrange Strain versus Cauchy Stress.

This plot allows us to clearly see the difference between the two measures and notice that for small values of strain, the difference becomes very small.

Conclusion

This chapter outlined the process and criteria for selecting the most suitable hyperelastic model for simulating the uniaxial stress response of an elastomer. Through rigorous simulation and analysis, the Ogden 3-term model was identified as the optimal choice for detailed and accurate modeling, supporting the project's goals and application requirements.

Chapter 4

Future Research and Conclusions

4.1 Future Research

While this study provided valuable insights into the modeling of elastomeric materials under uniaxial stress, several areas remain open for future investigation. One potential avenue for further research is exploring alternative material models that account for viscoelastic and time-dependent behaviors, which are critical for applications involving dynamic loading. The inclusion of temperature-dependent properties could also provide a more comprehensive understanding of elastomers in real-world environments where thermal factors affect material performance.

Another important area for future research is the multiaxial testing of elastomers, as the current study focused solely on uniaxial stress. Multiaxial tests, such as biaxial or shear testing, would provide a more complete set of data for validating hyperelastic models. Additionally, investigating non-homogeneous materials, including composites with elastomeric components, could extend the applicability of the simulation techniques developed in this study.

Lastly, future research could also focus on enhancing computational methods by applying more advanced techniques, such as machine learning algorithms for optimizing material parameter estimation and fitting processes. This would further reduce the gap between experimental results and predictive modeling, improving accuracy in a wider range of applications.

4.2 Conclusions

This study successfully modeled the deformation behavior of elastomer materials under uniaxial stress using non-linear FEA techniques in MSC Marc. Through a comprehensive comparison of different hyperelastic models—namely the Neo-Hookean, Mooney-Rivlin, and Ogden models—it was concluded that the Ogden 3-term model offered the highest accuracy in fitting experimental data and predicting material responses.

The use of uniaxial test data allowed for the effective calibration and validation of these models, demonstrating the importance of selecting the appropriate material model to accurately capture elastomer behavior under stress. The results underscore the significance

of non-linear analysis when working with materials that exhibit complex stress-strain relationships, such as elastomers.

This work provides a solid foundation for further advancements in elastomer modeling, particularly in the context of complex material behaviors and real-world engineering applications. The methodologies applied here can be expanded upon in future research to address the limitations identified, thus advancing the field of material modeling and contributing to more accurate and reliable engineering simulations.

References

- MSC Software Corporation,
MSC Marc User's Guide, Available at: <https://www.mscsoftware.com>.
- Keerthiwansa, R., Javorik, J., Kledrowetz, J., and Nekoksa, P., "Elastomer Testing: The Risk of Using Only Uniaxial Data for Fitting the Mooney-Rivlin Hyperelastic-Material Model", *Materials and Technologies*, 2018. DOI: 10.17222/mit.2017.085.
- Bathe, K.J., "Finite Element Procedures in Engineering Analysis", Available at: <https://soaneemrana.org>.
- Seymore, K.D., Domire, Z.J., DeVita, P., Rider, P.M., Kulas, A.S., "The Effect of Nordic Hamstring Strength Training on Muscle Architecture, Stiffness, and Strength", *European Journal of Applied Physiology*, 2017. DOI: 10.1007/s00421-017-3583-3.
- "Creep in Materials", Available at: <https://www.ae.msstate.edu>.
- Bradley, G.L., Chang, P.C., McKenna, G.B., "Rubber Modeling Using Uniaxial Test Data", *Journal of Applied Polymer Science*, Vol. 81, pp. 837–848, 2001. DOI: 10.1002/app.1503.
- Mooney, M.,
A Theory of Large Elastic Deformation, *Journal of Applied Physics*, 1940. Available at: <https://aip.scitation.org>.
- Treloar, L.R.G.,
- SINTEF, "Lecture on Finite Element Analysis", KMM Geilo 2012, Available at: <https://www.sintef.no>.